Int. J. Electrochem. Sci., 14 **(2019)** 585 – 597, doi: 10.20964/2019.01.63

International Journal of
ELECTROCHEMICAL
SCIENCE
www.electrochemsci.org

Electrochemical Oscillations during Copper Electrodissolution in Hydrochloric Acid Solution

Lifeng Ding[1,*] *, Zhengwei Song*[1]*, Peng Wu*[1]*, Jun Cheng*[2]*, Chongyan Chen*[2]*, Yulan Niu*[1]*, Bing Li*[1]

[1] Department of Chemistry and Chemical Engineering, Taiyuan Institute of Technology, Taiyuan 030008, PR China
[2] School of Chemical Engineering and Technology, North University of China, Taiyuan 030051, PR China
[*]E-mail: happydlf@163.com

Received: 24 June 2018 / *Accepted:* 4 September 2018 / *Published:* 30 November 2018

The electrodissolution process of copper anode is widely used in industrial copper-processing, such as electrolysis, electroplating, electrocatalysis, corrosion, and electric machining. Industrial electrochemical processes generally accompany spatiotemporal electrochemical oscillation (EO) phenomena. In this study, the mechanism of periodic EO in the Cu electro-oxidation of hydrochloric acid solution was systematically investigated through experimentation and simulation. The effect of scanning times, concentration of hydrochloric acid, mixing rate, temperature on the EO was studied by using CV, and the effect electric field was studied by current-time under constant potential and the single current step chronopotentiometry way. In theory, it established the reaction mechanism of the system and it was converted into three-variable mathematical model. So the EO was simulated by using Matlab. Theoretical simulation results were consistent with experimental ones. EO occurred as a result of the periodically alternating deposition and dissolution effects of white cuprous chloride deposited through the electro-oxidation of fresh Cu anode. These results provided insight into the relevance among the microchemical mechanisms of the macroscopic nonequilibrium phenomenon.

Keywords: Copper anode; Electrodissolution; Electrochemical oscillation; cyclic voltammetric

1. INTRODUCTION

The electrodissolution process of copper anode widely is used in electrolysis, electroplating, electrocatalysis, corrosion, and electric machining on the industrial copper-processing [1–6]. Industrial electrochemical process generally has high concentration, large current, mobility, and other characteristics, which are far from reaction equilibrium [7,8]. Elementary reaction steps of

EO are usually used in electrochemical systems, which gradually drive far from equilibrium via

an electric field, whereas nonlinear terms are significant and lead to spatiotemporal EO phenomena [9–11].

EO phenomenon, which occurs on the copper electrode in an electrochemical system, has long been reported. In 1957, Cooper et al. [12] determined that EO phenomenon occurs when copper anode is dissolved in HCl solution. They also speculated that oscillation occurs as a result of cyclical generation and dissolution of CuCl on Cu electrode surface. In 1985, Lee et al. [13] studied current oscillation that occurs on copper in acidic (H_2SO_4 or HCl) NaCl solution using rotating disk electrode. They determined that current oscillation occurs only when the generated CuCl film is sufficiently thick on the electrode surface, which is related to the diffusion of ion in the porous films. Cazares-Ibanez [14] studied the corrosion products formed at different potentials via recurrence plots. They determined that copper presents pitting corrosion character in different consistence solutions containing chloride and sulfate. They also determined that if the passivation layer is not sufficiently thick, then pitting phenomenon does not occur.

At present, the EO preliminary mechanism can be divided into three types. First, oscillation is formed by periodic deposition and dissolution of a material on the electrode surface. Second, oscillation is caused by cyclical changes of intermediate valence ions at the electrode interface. Third, oscillation occurs when bubbles are generated periodically on the electrode surface, and this phenomenon results in periodic variation of gains or losses of the electronic reaction to enable oscillation [15–17]. At present, the research of EO is limited to the discovery of phenomenon and the speculation of preliminary qualitative mechanism; however, the research on types and quantitative mechanism of EO in the actual different electrochemical system remains in the exploration [10]. This scenario greatly restricts the study on the phenomena and mechanism of EO. However, the study of EO phenomenon has important significance in theory. Some information of electrode reaction mechanism and the coupling nature among various elementary steps can be obtained from periodic EO behavior, which can be used to analyze quantitatively the reaction mechanism oscillation behavior to guide the practical application system [18–20].

In this study, the electrodissolution of copper anode in hydrochloric acid solution is considered the research subject on the basis of nonlinear nonequilibrium physical chemistry theory using the research methods of combination of experimental test and theoretical simulation. The dynamic behavior and characteristics of EO are explored to the internal mechanism of EO dynamic behavior in the electrolysis process. This study provides insights into the relevance among the microchemical mechanisms for the macroscopic nonequilibrium phenomenon. A new way to develop highly efficient copper production process in electrolytic refining and electric machining is also provided so on.

2. EXPERIMENTAL

All reagents were analytical grade. Water was purified using a water purification system (PALL Cascada II I 30, USA). Unless specially noted, the electrolyte contained HCl (0.2 $mol \cdot L^{-1}$). The electrolytic cell was placed in a heat collector constant temperature type magnetic stirrer (DF-101S, Shanghai, China) to maintain the constant temperature and stirring speed. Electrochemical tests were

conducted on an LK2005A electrochemical workstation (Tianjin Lanlike, China).

All experiments were performed in a thermostatic electrolytic cell with two-electrode system was employed in this experiment. For the two-electrode system, to simulate the industrial electrolysis, with a copper wire (0.5 mm in diameter, 4 mm in length, 99.95% purity) as working electrode and 304 stainless steel sheet (16 mm^2 effective area) as reference and counter electrodes, whose unreacted part was sealed with epoxy. The distance between the Cu anode and the stainless steel electrode is approximately 7.0 mm. All the electrodes were finely polished and cleaned in acetone and purified water. The scanning speed of the cyclic voltammetry (CV) was 50 $mV \cdot s^{-1}$. The morphology structure of the electrode surface was analyzed using optical metalloscopy (CDM-360C, Shanghai Dianying Optical Instrument).

3. RESULTS AND DISCUSSION

3.1 Effect of scanning time on EO

EO phenomenon significantly occurred on fresh copper anode in 0.2 $mol \cdot L^{-1}$ hydrochloric acid solution at 10 °C without mixing via cyclic voltammetric method. Figure 1a shows a full CV curve, the periodic oscillation appeared in the range of 1.5–2.5 V potential in the red line (oxidation). The CV curves were continuously scanned three different time to explore the effect of scanning time on EO in the Cu-HCl system. The different time of CV curves in 0.2 $mol \cdot L^{-1}$ hydrochloric acid solution were 6 min 30 s, 13 min, and 19 min 30 s, as shown in Figure 1a–1c. The CV curve of Figure 1a–1c were obtained by the same electrode scanning for 3 min. According to the comparison of Figure 1a–1c, when the reaction time was increased, oscillation signal weaken and then disappeared finally with reaction time increased. After the first cycle CV test, a layer of material was attached to the copper electrode surface. Then EO weakens or disappears by next CV test. Thus, the thickness of the precipitation film will affect the oscillation behavior. The key of oscillation experiment is that the electrode must be polished before each scanning CV.

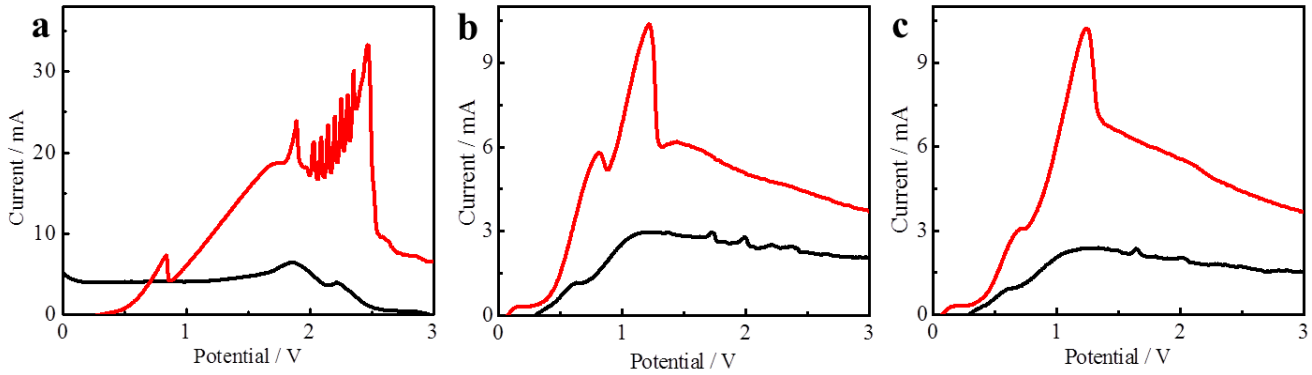

Figure 1. Effect of scanning time on cyclic voltammetry a: 6.5 min; b: 13 min; c: 19.5 min

3.2 Effect of hydrochloric acid's concentration on EO

The CV curves were tested in every experiment using fresh electrode at 10 °C without stirring to study the effect of concentration of hydrochloric acid on EO. The CV curves were tested in 0.1, 0.2, 0.3, 0.4, 0.5, 0.6 mol·L^{-1} hydrochloric acid solutions, respectively, the test results were shown in Figure2. Figure 2a shows the CV curve in 0.1 mol·L^{-1} hydrochloric acid solution, test potential range from 2 V to 3 V, thereby indicating a clear EO phenomenon. When the concentration of hydrochloric acid increased to 0.2 mol·L^{-1} in Figure 2b red line (oxidation), regular periodic oscillation appeared within the range of 1.5 V to 2.5 V, and its oscillation frequency was higher than that with 0.1 mol·L^{-1}. Figure 2c–2f show that oscillation disappeared with increased concentration from 0.3 mol·L^{-1} to 0.6 mol·L^{-1}. The peak width of the oxidation peak narrowed, and the peak height gradually lowered. As the concentration of hydrochloric acid increased, the oxidation reaction between 1 and 2.5 V decreased. It found that as the concentration of HCl increased, the concentration of [Cl^-] also increased. At the same time, the amount of Cu(Cl^-) on the anode also increased, which promoted the formation and dissolution of Cu(CuCl) on the electrode. Therefore, there would be an electrochemical oscillation. However, when the HCl concentration continued to increase, CuCl dissolved too quickly. It was difficult to observe the formation of Cu(CuCl) on the electrode surface, so the oscillation almost disappeared.

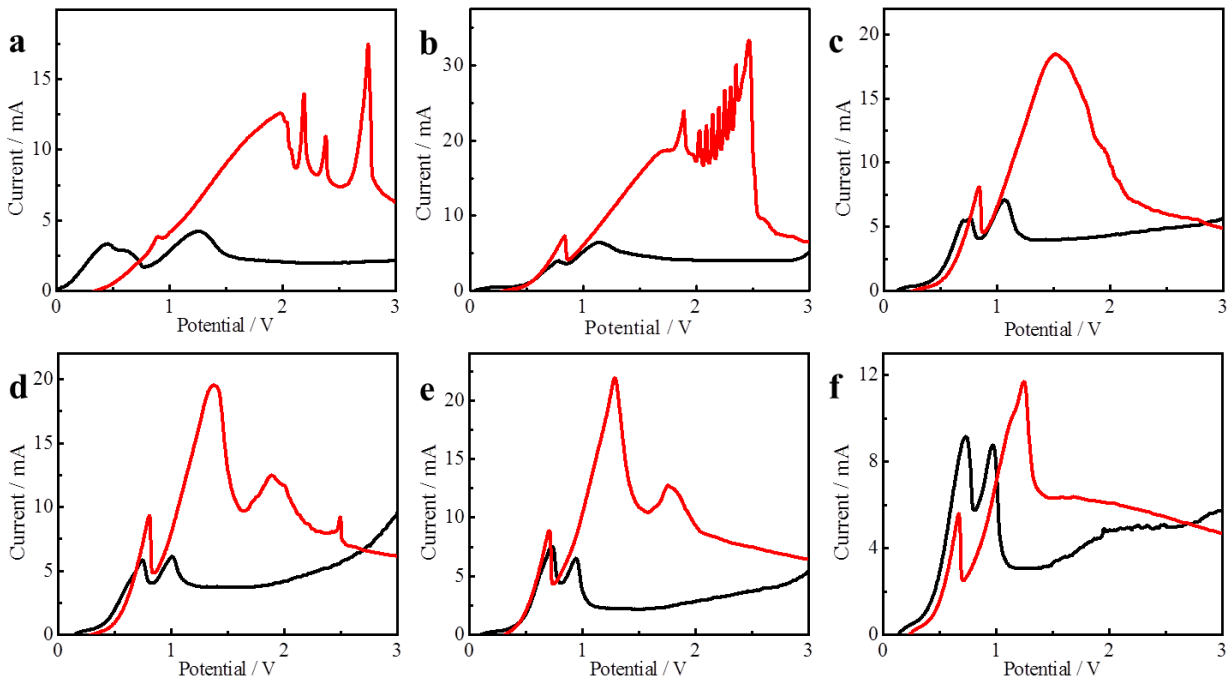

Figure 2. Effect of hydrochloric acid concentration on CV a: 0.1 mol·L^{-1}; b: 0.2 mol·L^{-1}; c: 0.3 mol·L^{-1}; d: 0.4 mol·L^{-1}; e: 0.5 mol·L^{-1}; f: 0.6 mol·L^{-1}

3.3 Effect of mixing rate on EO

The movement of ions in the electrolyte can also affect the behavior of EO, thus, CV curves with different mixing rates were tested using copper anode in hydrochloric acid electrolyte, as shown in Figure 3. These CV curves were tested in every experiment with fresh copper anode in 0.2 mol·L^{-1} hydrochloric

acid solution at 10 °C. The CV curves were tested with 0, 10, 20, 30, and 40 r·s^{-1} mixing rate. Figure 3a shows the CV curve without mixing and the regular periodic oscillation phenomenon that occurred in the potential range of 1.5–2.5 V in its red line (oxidation). Figure 3b shows that irregular little EO phenomenon occurred in the potential range of 1.5–2.5 V in the oxidation process when the mixing rate was 10 r·s^{-1}. The anodic peak obviously appeared only at approximately 2 V when the mixing rate increased to 20 r·s^{-1}, as shown in Figure 3c and oscillation trend existed. The oxidation peak around 2 V disappeared when the mixing rate continually increased to 30 or 40 r·s^{-1}. The comparison of Figure 3a–3e indicated that oscillation phenomenon gradually weakened or disappeared completely with the increase of mixing rate.

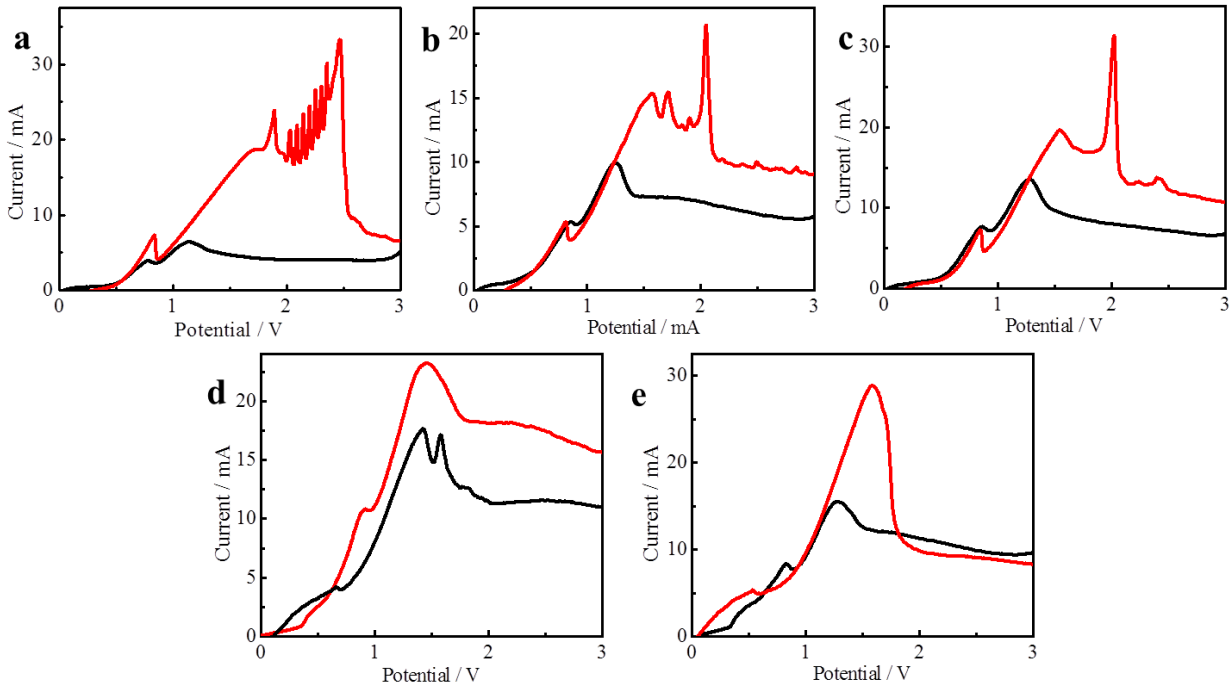

Figure 3. Effect of mixing rate on CV a: 0 r·s^{-1}; b: 10 r·s^{-1}; c: 20 r·s^{-1}; d:30 r·s^{-1}; e: 40 r·s^{-1}

The change of the electrode surface before and after oscillation were recorded using a camera as shown in Figure 4a and 4b, and the micro-topography of stainless steel surface was recorded using optical metalloscopy, as shown in Figure 4c and 4d.

The comparison of Figure 4a and 4b indicated that the working electrode was purple copper wire before the oscillation. Once the oscillation occurred, following a layer of white film on the copper electrode. As the film thickness increased, oscillation began to weaken or disappear. According to literature reports, forming a white precipitate of cuprous chloride on the copper anode in hydrochloric acid solution is easy [21,22]. Figure 4c shows the microsurface topography of cleanly polished stainless steel electrode, whose surface has linear stripes. After the oscillation was generated, the surface of the stainless steel sheet was obviously attached with some particles (as shown in Figure 4d). The color of deposited particles on the counter electrode was purple. To further analyze the white precipitate on the Cu electrode, it was magnified to obtain a high-magnification SEM image in Figures 4e and 4f. After the oscillation was generated, the precipitate on the surface of the electrode was irregularly layered about

2 μm thick. It was found by EDS analysis that the substance mainly contained Cu, Cl and O. The working copper electrode should be chloride and dissolved to copper ions, and then the copper ions were dissolved further to be transported to the counter electrode. High concentration of copper ions would transport to low concentration with mixing in the anode. A large number of copper ions were reduced to copper atoms by obtaining the electronics in the solution and those attached to the surface of the counter electrode. The oscillation would be reduced when copper ions were timely transported via dissolution of the anodic delivery. This scenario showed that mixing was not conducive to cause oscillation phenomenon for copper electrode in the hydrochloric acid. The EO was affected by concentration polarization. Hence, the concentration polarization was eliminated gradually by increase mixing rate in the system, and the oscillation phenomenon was weakened [23].

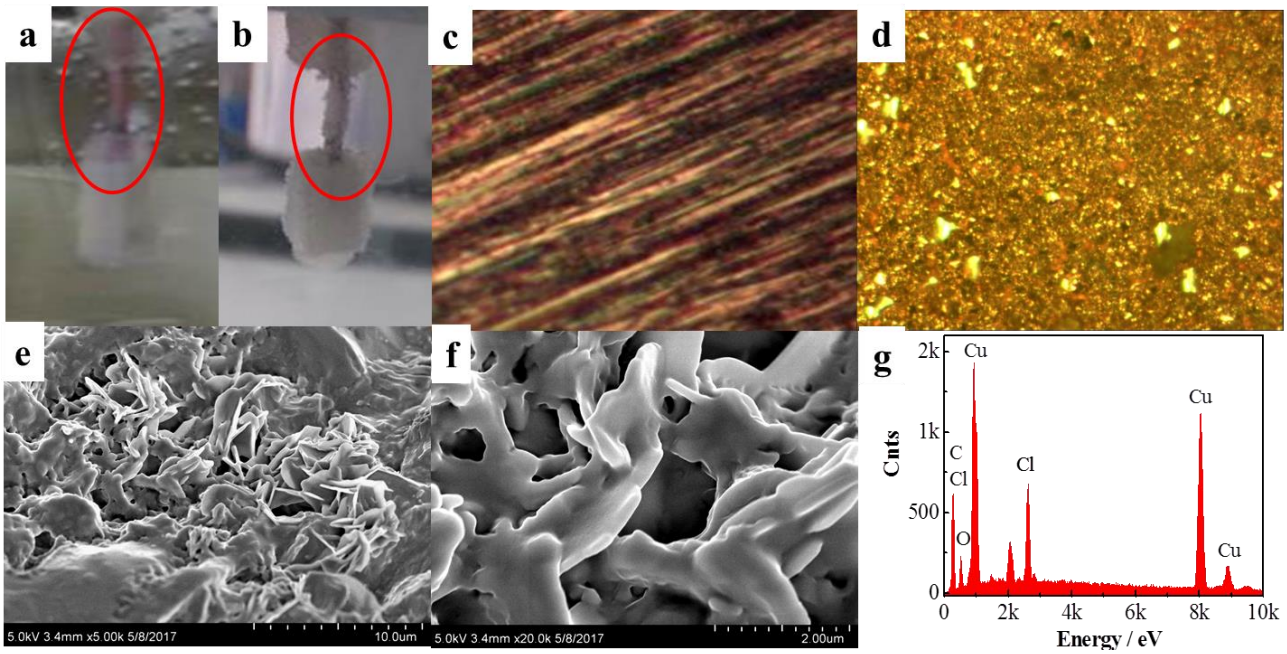

Figure 4. Electrode surface topography before and after the oscillation is generated a: photo of Cu electrode before oscillation; b: photo of Cu electrode after oscillation; c: microsurface topography of stainless steel electrode before oscillation; d: micro surface topography of stainless steel electrode after oscillation; e and f: SEM of the precipitate on Cu electrode after oscillation; g: EDS of the precipitate on Cu electrode after oscillation

3.4 Effect of temperature on EO

The temperature of electrolyte could also affect the EO behavior. These CV curves were tested in every experiment with fresh copper anode in 0.2 mol·L^{-1} hydrochloric acid solution without mixing. The CV test results at 10-45 °Cwere shown in Figure 5a–5d. Figure 5a shows the CV curve at 10 °C and the regular periodic oscillation phenomenon that occurred in the potential range of 1.5–2.5 V in its red line (oxidation). Figure 5b shows that irregular EO phenomenon occurred in the range of 2–2.5 V at 25 °C. The temperature increased continually to 35 °C, and the irregular EO phenomenon occurred faintly in the range of 1.5–2.5 V, as shown in Figure 5c. The oscillation completely disappeared in Figure

5d when the temperature reached 45 °C. The comparison of Figure 5a–5d showed that the oscillation gradually weakened or disappeared with the temperature gradually increased.. The white sediment was produced clearly on the copper anode at 10 °C during the experiment process, and the counter electrode did not change at the same time. Once the temperature increased to 45 °C, no white substances was produced on the copper anode, whereas the red substance was clearly and quickly covered on the surface of the counter electrode. White cuprous chloride precipitate was instable and easily decomposed in a high-temperature system, for example, hot water [24].Thus, this indicated the material on the working electrode is cuprous chloride. A large number of copper ions were reduced to copper. Then, they were attached to the surface of the stainless steel. This scenario showed that low temperature was beneficial to the regular periodic oscillation phenomenon for the copper–hydrochloric acid system, which had a direct relationship with cuprous chloride precipitated on the electrode surface.

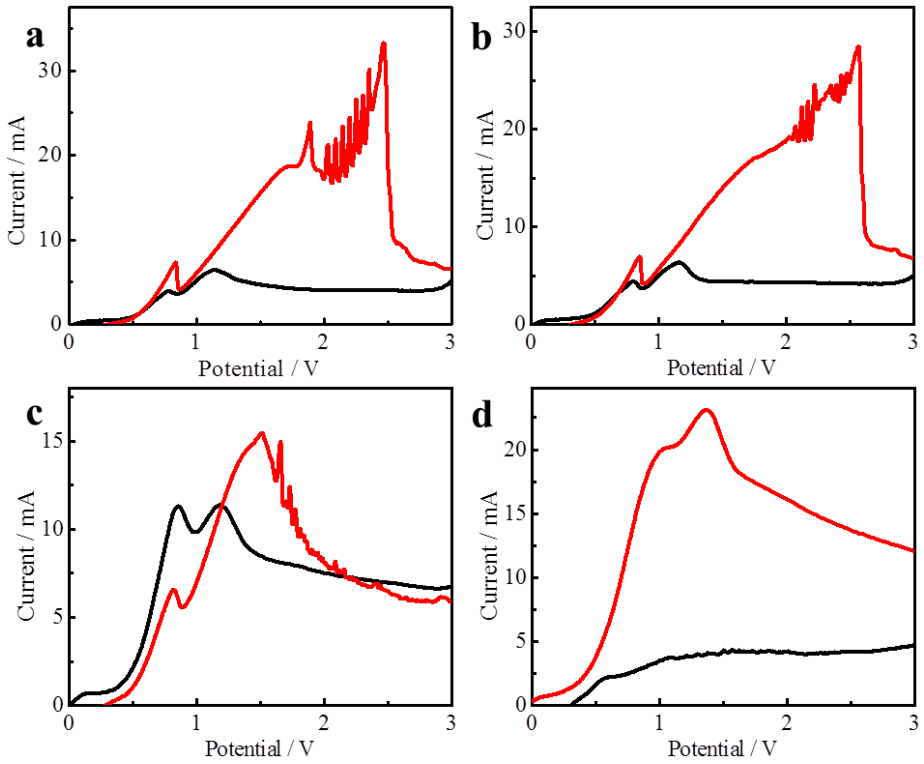

Figure 5. Effect of temperature on CV a: 10 °C, b: 25 °C, c: 35 °C, d: 45 °C

3.5 Effect of electric field on EO

The *I–t* curves were tested under constant potential conditions using electrochemical workstation. Second, the effect of electric field also included the effect of current on the EO. A series of E–t curves was tested under constant current conditions via the single current step chronopotentiometry way.

The *I–t* curves were tested at 2.10, 2.15, 2.20, 2.25, and 2.30 V in the copper–hydrochloric acid system, as shown in Figure 6a. When the potential was at 2.10 V, its current oscillation occurred in the range of 7–27 s, and the amplitude of oscillation was up to 25 mA. When the potential was at 2.15 V, its current oscillation occurred in the range of 8–18 s, and the amplitude of oscillation was up to 28 mA.

When the potential was at 2.20 V, its current oscillation occurred in the range of 5–15 s, and the amplitude of oscillation was up to 23 mA. When the potential was at 2.25 V, its current oscillation occurred in the range of 8–33 s, and the amplitude of oscillation was up to 20 mA. When the potential was at 2.30 V, its current oscillation occurred in the range of 5–30 s, and the amplitude of oscillation was up to 28 mA. The aforementioned effects of the potential on amplitude and oscillation range were summarized in Figure 6b. In the system, the effect of potential on amplitude was slightly evident. The time range of oscillation would be reduced and then increase with potential increased.

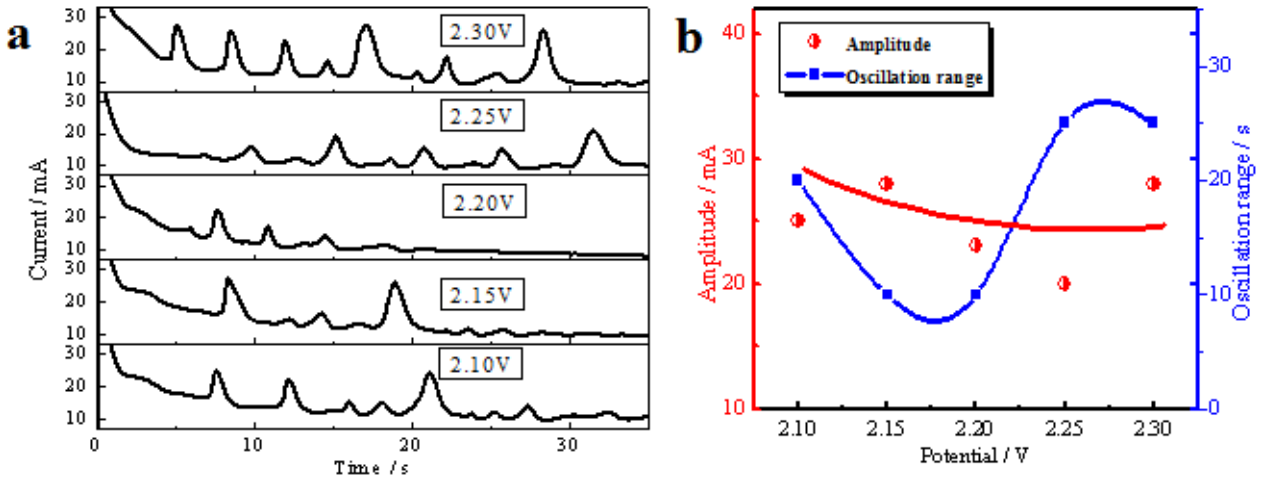

Figure 6. Effect of potential on EO a: *I–t* curves at different potentials; b: effect of potential on amplitude and oscillation range

The *E–t* curves were tested at 3, 5, 7, 13, and 19 mA in the copper–hydrochloric acid system, as shown in Figure 7a. When the current was 3 mA, regular periodic potential phenomenon occurred in the range of 75–100 s in its E–t curve. When the current was 5 mA, the regular periodic potential phenomenon occurred in the range of 30–40 s in its E–t curve. The comparison of the *E–t* curves of 3 and 5 mA indicated that both the starting time and endurance time of potential oscillation were shortened with increased current. The comparison of E–t curves under different currents indicated that when the current was low, the starting time of potential oscillation was late and its endurance time was long because of the slow speed of reactions on the electrode surface. When the current was hight, the starting time of potential oscillation was early and its endurance time was long because of the fast speed of reactions.

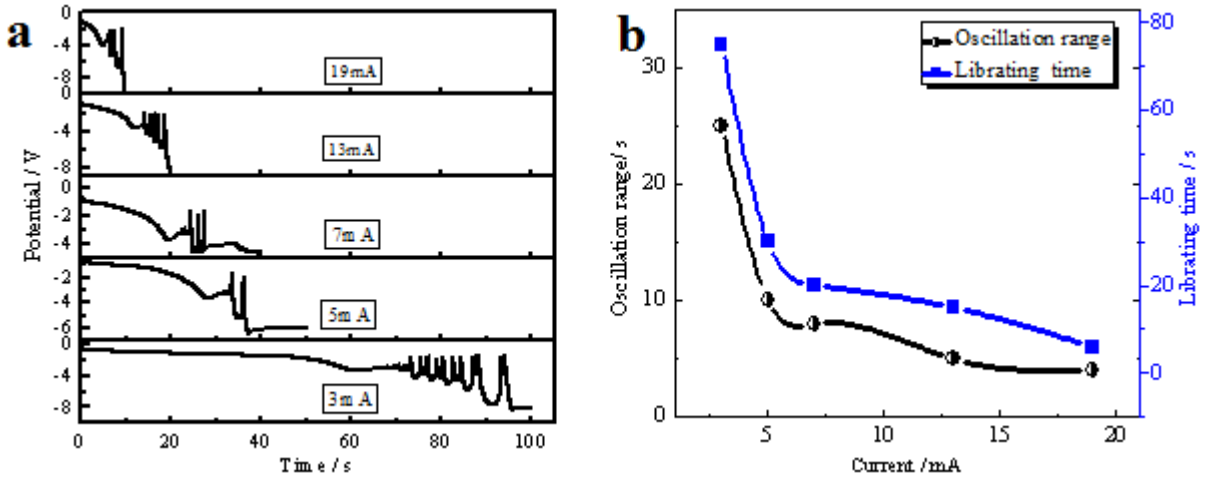

Figure 7. Effect of current on EO a: *E–t* curves at different currents; b: effect of current on amplitude and oscillation range

3.6 Mechanism of EO

Similar redox reactions have been reported in the studies on the reaction between Cu^+ and Cl^-. During oxidization, several possible intermediates are produced, such as H^+, Cu, Cu^+, Cl^-, CuCl, and $CuCl_2^-$, where CuCl is deposited on the Cu anode to form Cu(CuCl), and Cl^- is adsorbed on the Cu anode to form Cu(Cl^-) [21,22,24]. These intermediates react with one another and finally produce Cu^+. According to Prigogine's theory [25], the deposition and dissolution effect of Cu(CuCl) deposited by the electro-oxidation of Cu anode may provide essential nonlinear items for the mechanism of EO. Possible electrochemical reactions are summarized as follows [12,26]:

$$Cu - e \xrightarrow{k_1} Cu^+ \quad (1)$$

$$Cu + Cl^- \xrightarrow{k_2} Cu(Cl^-) \quad (2)$$

$$Cu^+ + Cu(Cl^-) \xrightarrow{k_3} Cu(CuCl) \quad (3)$$

$$Cu(Cl^-) + Cu(Cl^-) - e \xrightarrow{k_4} Cu(CuCl) + Cl^- \quad (4)$$

$$Cu(CuCl) + Cu(Cl^-) \xrightarrow{k_5} CuCl_2^- + 2Cu \quad (5)$$

where Cu is the reaction surface without a film of CuCl salt; Cu(CuCl) is the electrode surface with a CuCl film covering the Cu anode surface; Cu^+ and Cl^- represent cuprous ion and chloride ion adjacent to the electrode surface; k_1, k_2, k_3, k_4, and k_5 are rate constants.

During the dissolution of the Cu anode, the concentration of Cu^+ adjacent to the electrode surface may change because of electrode dissolution and may be transported to the solution bulk. Consequently, the potential of the diffusion part of the double layer changes with increased concentration of the Cu^+ ion; thus, it influences the rate of the electrode dissolution reaction. This coupling may result in a full dynamic behavior.

[Cl^-] is assumed as constant C in bulk to simplify the buildup of the nonlinear dynamic behavior. Following the model, let θ be the amount of crystalline Cu(CuCl) that covered the anode surface; therefore, (1–θ) is the coverage of the Cu anode surface without the Cu(CuCl) film; *x* is [Cu(Cl^-),] and y is [Cu^+] adjacent to the electrode surface. The evolution equation of the anodic electrochemical system

is described as follows [27,28]:

$$\frac{dx}{dt} = k_2c(1-\theta) - k_3xy - k_4x^2 - k_5x\theta \quad (6)$$

$$\frac{dy}{dt} = k_1(1-\theta) - k_3xy \quad (7)$$

$$\frac{d\theta}{dt} = k_3xy + k_4x^2 - k_5x\theta \quad (8)$$

letting,

$$f(x, y, \theta) = k_2c(1-\theta) - k_3xy - k_4x^2 - k_5x\theta \quad (9)$$

$$g(x, y, \theta) = k_1(1-\theta) - k_3xy \quad (10)$$

$$h(x, y, \theta) = k_3xy + k_4x^2 - k_5\theta x \quad (11)$$

If (X_0, Y_0, θ_0) is the steady-state solution of dynamic Eqs. (9), (10), and (11) when f(X_0, Y_0, θ_0) = 0, g(X_0, Y_0, θ_0) = 0 and h(X_0, Y_0, θ_0) = 0, then (X_0, Y_0, θ_0) can be solved.

Let $X = X_0 + x$, $Y = Y_0 + y$, $\theta = \theta_0 + \theta$, (x is the perturbation variable around X_0; y is the perturbation variable around Y_0; and θ is the perturbation variable around θ_0). Eqs. (9), (10), and (11) can be expanded around the steady state (X_0, Y_0, θ_0) based on Taylor series expansion. After ignoring the high-order terms, the linear perturbation equations can be written as follows [10,18]:

$$\delta x/\delta t = a_{11}x + a_{12}y + a_{13}\theta + D_x\nabla^2 x \quad (12)$$

$$\delta y/\delta t = a_{21}x + a_{22}y + a_{23}\theta + D_y\nabla^2 y \quad (13)$$

$$\delta \theta/\delta t = a_{31}x + a_{32}y + a_{33}\theta + D\theta\nabla^2\theta \quad (14)$$

$$\begin{bmatrix} a_{11} = \partial f/\partial X\big|_{X_0,Y_0,\theta_0}; & a_{12} = \partial f/\partial Y\big|_{X_0,Y_0,\theta_0}; & a_{13} = \partial f/\partial\theta\big|_{X_0,Y_0,\theta_0} \\ a_{21} = \partial g/\partial X\big|_{X_0,Y_0,\theta_0}; & a_{22} = \partial g/\partial Y\big|_{X_0,Y_0,\theta_0}; & a_{23} = \partial g/\partial\theta\big|_{X_0,Y_0,\theta_0} \\ a_{31} = \partial h/\partial X\big|_{X_0,Y_0,\theta_0}; & a_{32} = \partial h/\partial Y\big|_{X_0,Y_0,\theta_0}; & a_{33} = \partial h/\partial\theta\big|_{X_0,Y_0,\theta_0} \end{bmatrix} \quad (15)$$

The Jacobian matrix for the equations takes the following form by substituting Eqs. (9), (10) and (11) into Eq. (15):

$$\begin{bmatrix} a_{11} = -k_3y_0 - 2k_4x_0 - k_5q_0; & a_{12} = -k_3x_0; & a_{13} = -k_2c - k_5x_0; \\ a_{21} = -k_3y_0; & a_{22} = -k_3x_0; & a_{23} = -k_1; \\ a_{31} = k_3y_0 + 2k_4x_0 - k_5q_0; & a_{32} = k_3x_0; & a_{33} = -k_5x_0; \end{bmatrix} \quad (16)$$

The characteristic equation of the Jacobian matrix is as follows:

$$\lambda^3 - T\lambda^2 + \delta\lambda - \gamma = 0 \quad (17)$$

where

$$T = a_{11} + a_{22} + a_{33} \quad (18)$$

$$\delta = a_{11}a_{22} - a_{12}a_{21} + a_{22}a_{33} - a_{23}a_{32} + a_{21}a_{33} - a_{31}a_{13} \quad (19)$$

$$\gamma = a_{11}a_{22}a_{33} + a_{21}a_{32}a_{13} + a_{31}a_{23}a_{12} - a_{31}a_{22}a_{13} - a_{23}a_{32}a_{11} - a_{33}a_{21}a_{12} \quad (20)$$

Following the Routh–Hurwitz theorem, one of the following conditions results in system instability [18].

$$T > 0,\ \gamma > 0,\ T\delta - \gamma > 0 \quad (21)$$

According to calculations, $T < 0$, $\gamma < 0$; therefore, $T\delta - \gamma > 0$ is the condition necessary for instability. According to the simulation results of Hausse, a stable limit cycle of oscillation can appear in the presence of two complex roots for the characteristic equation and $T\delta - \gamma > 0$.

Current oscillation can occur in the aforementioned systems presented beyond the Hopf bifurcation. Total current is determined by electro-oxidation reactions (1) and (4). The total current density J_0 can be written as follows [11,29]:

$$J_0 = \sum J_i = \sum nF_{(\Phi_{DL})} c_{(\Phi_{DL})} k_{(\Phi_{DL})} = Fk_1 + Fk_4 X^2 \qquad (22)$$

where X is a function of k and time. After comparing the theoretical modeling and experimental tests, the links between parameters can be determined. The parameter k is related to potential, concentration, temperature, and time.

Time–current oscillation curve can be theoretically calculated, provided that suitable kinetic parameters are available. A simulated time–current oscillation curve of J_0 is calculated to prove the proposed mechanism for the origin of oscillation. However, obtaining the precise value of every kinetic constant at a specific anode potential is difficult. Approximate kinetic constants can then be estimated to elucidate the preliminary mechanism of the origin of oscillation.

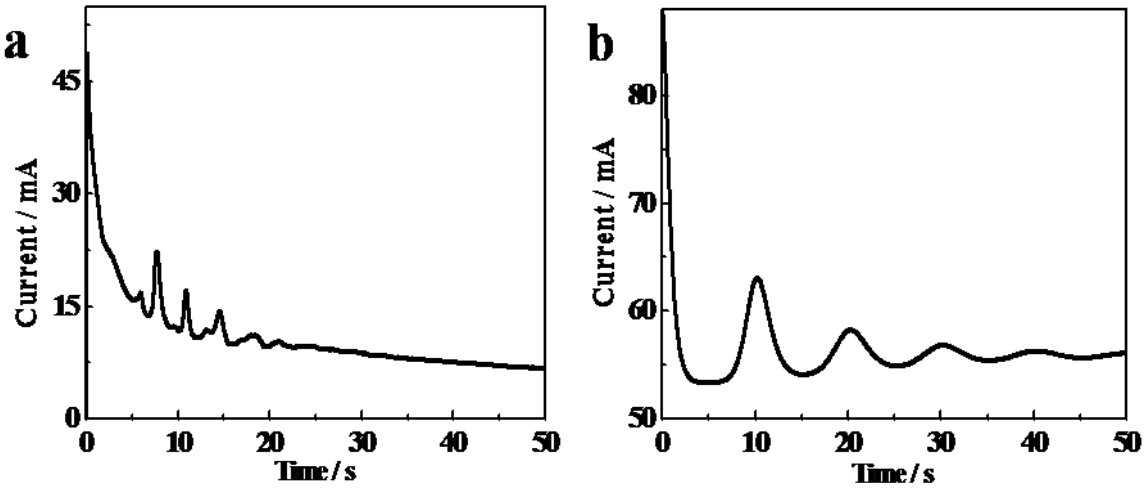

Figure 8. (a) When $[H^+]$ = 0.20 mol/L and [HCl] = 0.2 mol/L, I-t curve of current oscillation; (b) A calculated time–current curve (C=0.2 $mol \cdot L^{-1}$; k_1=2.75 $mol \cdot L^{-1} \cdot s^{-1}$; k_2=2×10^{-7} s^{-1}; k_3=9.99×10^{-2} $mol^{-1} \cdot L \cdot s^{-1}$; k_4=5×10^{-3} s^{-1}; k_5=5×10^5 $mol^{-1} \cdot L \cdot s^{-1}$).

A typical oscillation curve can be calculated (Figure 8b), if $C = 0.2$ $mol \cdot L^{-1}$; $k_1 = 2.75$ $mol \cdot L^{-1} \cdot s^{-1}$; $k_2 = 2 \times 10^{-7}$ s^{-1}; $k_3 = 9.99 \times 10^{-2}$ $mol^{-1} \cdot L \cdot s^{-1}$; $k_4 = 5 \times 10^{-3}$ s^{-1}; $k_5 = 5 \times 10^{-5}$ $mol^{-1} \cdot L \cdot s^{-1}$. The results derived from this simplified model agree with the experimental results shown in Figure 8a for amplitude and frequency. Furthermore, the shape of the oscillation curve minimally differs between the theoretical simulation and the experiment because of the slow capacitor discharge relaxation caused by the electric double layer. Nevertheless, the effect of capacity on the waveform must be further investigated.

4. CONCLUSIONS

Regular periodic EO phenomenon occurred in the CV curve for the fresh copper electrode in 0.2 $mol \cdot L^{-1}$ HCl solution at 10 °C without mixing. The EO occurred as a result of the periodically alternating

deposition and dissolution effects of white cuprous chloride deposited through electro-oxidation of the fresh Cu anode. Cuprous chloride precipitate was precarious and easily decomposed in hot water; thus, the EO gradually weakened with increased temperature. The concentration polarization was eliminated by mixing, thereby promoting the transfer of copper ions; thus, the EO gradually weakened when the mixing rate was great. When the potential was large, the range of EO in the I–t curve was great. When the current was large, the starting time of potential oscillation was early and its endurance time was short. In theory, the reaction mechanism of the system was established, and it was converted into three-variable mathematical model. Thus, the EO was simulated using MATLAB. The theoretical simulation results are consistent with the experimental results. This study provided insights into the relevance between the microchemical mechanisms for the macroscopic nonequilibrium phenomenon. A new way to develop highly efficient copper production process in electrolytic refining and electric machining was also provided.

ACKNOWLEDGMENTS
This work was supported by the National Natural Science Foundation of China (NSFC51604180), the Applied Basic Research Programs of Science and Technology Department of Shanxi Province (201701D221036), the start-up funds of Taiyuan Institute of Technology, and the Youth Academic Leader of Taiyuan Institute of Technology support program.

References

1. B. Im, S. Kim, *Electrochim. Acta*, 130(2014) 52-59.
2. D. Schab, K. Hein, *Can. Metall. Quart.*, 31(2013) 173-179.
3. D. Ihara, T. Nagai, R. Yamada, S. Nakanishi, Electrochim Acta 55(2009) 358-362.
4. D. Josell, T. P. Moffat, *J. Electrochem. Soc.*, 161(2014) D558-D563.
5. L. F. Ding, F. Liu, J. Cheng, Y. L. Niu, *J. Appl. Electrochem.*, 48 (2018) 175-185.
6. M. H. Abdel-Aziz, I. Nirdosh, G. H. Sedahmed, *J. Taiwan Inst. Chem. E*, 45 (2014) 840-845.
7. X. Fan, D. P. Yang, L. F. Ding, J. Du, Z. H. Liu, C. Y. Tao, *Chemphyschem,* 16 (2015) 176-180.
8. L. F. Ding, Y. X. Yang, L. F. Liao, J. Du, Y. D. Wang, X. Fan, C. Y. Tao, *J. Electrochem. Soc.*, 163 (2016) E70-E74.
9. K. Kamiya, K. Hashimoto, S. Nakanishi, *Chem. Phys. Lett.*, 530 (2012) 77-80.
10. X. Fan, J. Hou, D. G. Sun, S. Y. Xi, Z. H. Liu, J. Du, J. L. Luo, C. Y. Tao, *Electrochim Acta,* 102 (2013) 466-471.
11. M. F. Cabral, R. Nagao, E. Sitta, M. Eiswirthbc, H. Varela, *Phys. Chem. Chem. Phys.,*15 (2013) 1437-1442.
12. R. S. Cooper, J. H. Bartlett, *J. Electrochem. Soc.*, 105 (1957) 109-116.
13. H. P. Lee, K. Nobe, A. J. Pearlstein, *J. Electrochem. Soc.*, 132 (1985) 1031-1037.
14. E. Cazares-Ibáñez, G. AVázquez-Coutiño, E. García-Ochoa, *J. Electroanal. Chem.*, 583 (2005) 17-33.
15. J. Eskhult, C. Ulrich, F. Bjorefors, L. Nyholm, *Electrochim Acta*, 53(2008) 2188-2197.
16. N. T. M. Hai, J. Odermatt, V. Grimaudo, K. W. Kramer, A. Fluegel, M. Arnold, D. Mayer, P. Broekmann, *J. Phys. Chem. C*, 116 (2012) 6913-6924.
17. W. B. Ni, T. Q. Liu, R. Guo, Acta Phys-Chim. Sin., 22 (2006) 502-506.
18. D. Y. Hua, J. L. Luo, *Chem. Phys. Lett.*, 299 (1999) 345-351.
19. I. Z. Kiss, V. Gaspar, L. Nyikos, P. Parmananda, *J. Phys. Chem. A*, 101 (1997) 8668-8674.

20. I. Z. Kiss, Z. Kazsu, V. Gáspár, *Chaos*, 16 (2006) 033109.
21. Y. T. Lin, J. W. Ci, W. C. Tu, W.Y. Uen, S. M. Lan, *Thin Solid Films*, 591 (2015) 43-48.
22. D. M. Bittner, D. P. Zaleski, S. L. Stephens, D. P. Tew, N. R. Walker, *J. Chem. Phys.*, 142 (2015) 1-10.
23. H. Yang, R. G. Reddy, *Electrochim Acta*, 178 (2015) 617-623.
24. B. Yin, S. Zhang, X. Zheng, F. Qu, X. Wu, *Nano-Micro Lett.*, 6 (2014) 340-346.
25. I. Prigogine, D. Kondepudi, *John Wiely & Sons Inc*, (2015).
26. M. Itagaki, T. Mori, K. Watanabe, *Corros. Sci.*, 41 (1999) 1955-1970.
27. S. L. Chen, N. Trish, S. Mark, *T. I. Met. Finish*, 104(2000) 6791-6798.
28. R. Nagao, I. R. Epstein, E. R. Gonzalez, H. Varela, *J. Phys. Chem. A*, 112 (2008) 4617-4624.
29. J. Keizer, D. Scherson, *J. Phys. Chem*, 84 (1980) 2025-2032.